



UNIVERSITY OF  
GLOUCESTERSHIRE

This is a peer-reviewed, post-print (final draft post-refereeing) version of the following published document and is licensed under Creative Commons: Attribution-Noncommercial-No Derivative Works 4.0 license:

**Mohammed, Fiyaz, Stones, Daniel H ORCID logoORCID:  
<https://orcid.org/0000-0002-8981-7943> and Willcox, Benjamin  
E. (2019) Application of the immunoregulatory receptor  
LILRB1 as a crystallisation chaperone for human class I MHC  
complexes. *Journal of Immunological Methods*, 464. pp. 47-56.  
doi:10.1016/j.jim.2018.10.011**

Official URL: <https://doi.org/10.1016/j.jim.2018.10.011>

DOI: <http://dx.doi.org/10.1016/j.jim.2018.10.011>

EPrint URI: <https://eprints.glos.ac.uk/id/eprint/6148>

#### **Disclaimer**

The University of Gloucestershire has obtained warranties from all depositors as to their title in the material deposited and as to their right to deposit such material.

The University of Gloucestershire makes no representation or warranties of commercial utility, title, or fitness for a particular purpose or any other warranty, express or implied in respect of any material deposited.

The University of Gloucestershire makes no representation that the use of the materials will not infringe any patent, copyright, trademark or other property or proprietary rights.

The University of Gloucestershire accepts no liability for any infringement of intellectual property rights in any material deposited but will remove such material from public view pending investigation in the event of an allegation of any such infringement.

PLEASE SCROLL DOWN FOR TEXT.

# Application of the immunoregulatory receptor LILRB1 as a crystallisation chaperone for human class I MHC complexes

Fiyaz Mohammed<sup>a,1</sup>, Daniel H. Stones<sup>a,b,1</sup>, Benjamin E. Willcox<sup>a,\*</sup>

<sup>a</sup>Cancer Immunology and Immunotherapy Centre, Institute of Immunology and Immunotherapy, University of Birmingham, Edgbaston, Birmingham B15 2TT, UK

<sup>b</sup>School of Natural and Social Science, University of Gloucestershire, Cheltenham, GL50 4AZ, UK

\* Corresponding author.

<sup>1</sup> These authors contributed equally to this study.

## 1. Introduction.

A molecular understanding of the class I MHC molecule has been pivotal in deciphering its central role in T cell immunity. From the initial descriptions of class I MHC architecture (Bjorkman et al., 1987), which highlighted a highly polymorphic groove containing electron density corresponding to bound antigen peptides, structural analyses of pMHC complexes, to date still predominantly focussed on X-ray crystallographic approaches, have led the way in our efforts to understand MHC function. While these have established fundamental molecular principles underlying peptide antigen presentation and T cell recognition (Madden, 1995), structural studies of pMHC molecules continue to provide major insights into the critical role of antigenic peptides in disease pathogenesis (Illing et al., 2012; Ostrov et al., 2012), immunotherapeutic strategies (Hoppe et al., 2014; Madura et al., 2015) and into poorly understood aspects of T cell recognition, such as posttranslationally modified peptides (Mohammed et al., 2008, 2017; Petersen et al., 2009).

Despite the advent of recombinant methods, availability of extended screens, introduction of crystallisation nanovolume robotics and dramatic technological advances in synchrotron radiation sources, the requirement to overcome the “crystallisation bottleneck” is still a significant impediment to such X-ray crystallographic analyses of pMHC (Warke and Momany, 2007). Consequently, reliably achieving structure determinations for predefined pMHC targets can be challenging, a fact exacerbated by the huge diversity of MHC alleles and antigenic peptides of interest. In addition to standard crystallisation techniques such as sparse matrix sampling and seeding techniques (Bulek et al., 2012), a number of novel strategies are available to facilitate crystallisation of challenging proteins, including the surface-entropy reduction approach (Derewenda, 2010) involving substitution of lengthy side chains with Ala, Ser, His and Tyr, and chemical modification of Lys residues by reductive methylation (Walter et al., 2006). These clearly have proven utility but are not successful for every protein, and also have the potential to interfere with the delicate chemistry of the biologically critical class I MHC antigen-binding groove. An alternative is the use of non-covalent crystallisation protein chaperones (Bukowska and Grütter, 2013). This approach involves co-crystallising a target protein, such as an antibody fragment, and can

promote crystallisation by reducing target conformational heterogeneity and providing an additional surface for crystal contacts (Griffin and Lawson, 2011). While superficially appealing, it is unclear how this approach could best be applied to pMHC molecules.

Post-translationally modified peptides have emerged as an important group of antigens relevant to both autoimmunity and cancer. Phosphorylated peptides are increasingly recognised as promising tumour-associated antigens (Mohammed et al., 2017; Zarlino et al., 2000; Depontieu et al., 2009; Cobbold et al., 2013) and recent studies have focused on establishing the molecular ground rules for phosphopeptide presentation by class I MHC molecules (Mohammed et al., 2008; Petersen et al., 2009). Our own initial molecular studies in this area, which focussed on peptides bearing phosphorylations at P4 (so called “canonical” phosphorylations, the most prevalent in the HLA-A2-restricted phosphopeptide repertoire), outlined clearly how the P4 phosphate moiety can mediate energetically significant contacts to positively charged MHC residues, while remaining highly prominent within the antigen-binding groove, and available for TCR recognition. Based on these findings the phosphate was defined as a novel “phosphate surface anchor” (Mohammed et al., 2008).

Subsequent to these studies, we sought to address two outstanding questions in phosphopeptide immunology: firstly, how conformationally distinct phosphopeptide antigens are compared to their non-phosphorylated counterparts (Mohammed et al., 2017) – an issue highly relevant for therapeutic targeting of phosphopeptide antigens, and secondly, how peptides bearing phosphorylations at positions other than P4 are accommodated in the MHC antigen binding groove – about which only very limited structural data are available. We prioritised structural studies on a range of specific pMHC complexes to address these questions, which focussed on both non-phosphorylated counterparts of previously structurally analysed P4 phosphopeptides and phosphopeptides bearing “non-canonical” (i.e. non-P4) phosphorylations. However, difficulties in crystallising both of these classes of pMHC complexes led us to explore different approaches to circumvent this problem.

This study describes a non-covalent crystallisation chaperone methodology to efficiently facilitate crystallisation of pMHC molecules, which exploits a natural ligand interaction involving LILRB1. This strategy has been applied to both conventional and post-translationally modified peptide-HLA-A2 complexes that were recalcitrant to crystallisation, facilitating both crystallisation and structure determination. This provides a new approach to catalyse molecular studies of immunobiologically important pMHC complexes. Although our results focus on HLA-A2, LILRB1 is an immunoregulatory receptor that binds a diverse range of classical (HLA-A, HLA-B and HLA-C) and non-classical (HLA-E, HLA-F and HLA-G) MHC molecules (Chapman et al., 1999; Willcox et al., 2003; Dulberger et al., 2017; Jones et al., 2011), highlighting the potential of the method to be applied to a wider range of class I MHC molecules.

Table 1 Crystallisation trials for HLA-A2 molecules bound to non-canonical or non-phosphorylated peptides in the presence (dark grey)/absence (light grey) of LILRB1-Values in parentheses represent the number of crystallisation hits observed. Source Proteins: LSP1 - Lymphocyte Specific Protein1, POF1B - Premature Ovarian failure 1B, PKD2 - Protein Kinase D2, N4BP2 - Nedd4 binding protein 2, AMPD2 - adenosine monophosphate deaminase 2, BCAR3 - Breast cancer anti-estrogen resistance 3, RPS17 - Ribosomal Protein S17, CHEK1 - Checkpoint kinase 1, PLEKHA6 - Pleckstrin homology domain-containing family A member 6, HSP27 - Heat Shock Protein 27, RETREG2 - Reticulophagy regulator 2, TRAPPC1 - Trafficking protein particle complex subunit 1, PLEKHA6 -Phosphoinositol 3-phosphate binding protein and TAF13 - TFIID transcription initiation factor subunit 13. Commercial Screens: Molecular dimensions (Structure screen 1 + 2, Pact, ProPlex, BCS and JCSG+), Hampton Research (PEG/Ion, Index and PEG Rx) and Emerald Biosystems (Wizard 1–4). Generic LILRB1-pHLA-A2 crystallisation conditions: PAT (20% PEG 3350, Ammonium 0.2 M acetate and 0.1 M Tris-HCl pH 8.5) and PAH (20% PEG 3350, 0.2 M ammonium acetate and 0.1 M HEPES pH 7.4).

Epitope	Source protein	Commercial screens (no of crystallisation hits)	Total hits	Collection	Screening with LILRB1 (no of crystallisation hits)	Total hits	Collection
RQASIELPSMAV	LSP1	JCSG <sup>+</sup> (1), Wizard 1 + 2, Pact, PEG/Ion, and Index (1)	2	No	Proplex (8) and PAH (1)	9	2.7 Å
RQASIELPSM	LSP1	JCSG <sup>+</sup>	0	n/a	Not screened	–	–
RTYSGPMNKV	POF1B	PEG/Ion, Structure Screen 1 + 2, JCSG <sup>+</sup> and Index	0	n/a	PAT (1)	1	Yet to be optimised
RQASLSISV	PKD2	JCSG <sup>+</sup> , BCS (1) and Wizard 1 + 2	1	1.9 Å	–	–	–
KMDSFLDMQL	N4BP2	Index, JCSG <sup>+</sup> , PEG/Ion (1), pact and wizard 1 + 2	1	No	PAT/PAH (2), PEG Rx (3), JCSG <sup>+</sup> (Madden, 1995), PEG/Ion (4) and Structure Screen 1 + 2 (1)	12	Yet to be optimised
RQISQDVKL	AMPD2	PEG/Ion (3), Pact (1), Index and BCS	4	2.1 Å	–	–	–
IMDRpTPEKL	BCAR3	JCSG <sup>+</sup> , PEG/Ion, Structure Screen 1 + 2, Index (1), Pact and BCS	1	No	PAT/PAH (1)	1	Yet to be optimised
KLLDFGSLpSNLQV	RPS17	JCSG <sup>+</sup> , PEG/Ion, Structure Screen 1 + 2 (1), Index and Pact	1	No	PAT	0	–
KLIDIVpSSQKV	CHEK1	PEG/Ion, Pact, JCSG <sup>+</sup> , Index and BCS	0	n/a	PAT (1)	1	Yet to be optimised
SMpTRSPPRV	SRp46 splicing factor	BCS	0	n/a	Not screened	–	–
SLQPRSHpSV	PLEKHA6	BCS	0	n/a	Not screened	–	–
RQLSSGVSEI	HSP27	Pact (1), Index (2) and PEG/Ion (5)	8	No	Not screened	–	–
RLSSPLHFV	RETREG2	PEG/Ion, Index, Pact, Structure Screen 1 + 2 and BCS	0	n/a	PAT/PAH (1) and PEG/Ion (20)	21	3.2 Å
RLQSTSERL	Mitochondrial escape 1-like 1	Wizard 1–4 (1), JCSG <sup>+</sup> , Pact and BCS	1	No	PEG/Ion	13	2.8 Å
RTLSHISEA	FLJ13725	JCSG <sup>+</sup> , Structure Screen 1 + 2, Index, ProPlex (1), Wizard 1–4 (1), PEG/Ion and BCS	2	No	Not screened	–	–
RTFSPTYGL	β-synemin/Desmulin	PACT, JCSG <sup>+</sup> , Structure Screen 1 + 2, Index, Wizard 1–4, PEG Rx, PEG/Ion and BCS	0	n/a	PAT/PAH (1), PEG Rx (2), JCSG <sup>+</sup> (2) and PEG/Ion (5)	10	2.3 Å
RLDSYVRSL	TRAPPC1	Index, JCSG <sup>+</sup> , PEG/Ion, Pact, PEG Rx, Wizard 1 + 2 and BCS	0	n/a	Not screened	–	–
RLFSKELRC	TAF13	PEG/Ion, Wizard 1 + 2 and Pact	0	n/a	Not screened	–	–

## 2. Materials and methods.

### 2.1 Cloning, expression and purification

The recombinant clones of the LILRB1 D1D2 region (residues 24–221 of the mature protein; hereafter referred to as LILRB1) and HLA-A2 were prepared as previously reported (expression constructs will be made available upon request) (Willcox et al., 2003). High levels of pHLA-A2 complexes (comprising residues 25–300 of the mature A2 heavy chain, non-covalently associated with  $\beta$ 2M and peptide) and LILRB1 were produced using conventional methods involving expression in *Escherichia coli* and in vitro dilution refolding (Garboczi et al., 1992). Renatured LILRB1 and pHLA-A2 complexes were concentrated independently, and purified by size-exclusion chromatography using a Superdex 200 column.

### 2.2 Crystallisation, data collection and processing

HLA-A2 molecules in complex with non-P4 phosphorylated and non-phosphorylated epitopes were screened against commercially available crystallisation conditions with the Mosquito nanolitre robot (TTP Labtech) using the vapour diffusion method (Table 1). Alternative crystallisation strategies involving LILRB1 were performed using a 1:1 stoichiometric mixture of purified LILRB1 and pHLA-A2 at 10–14 mg/ml. Diffraction-grade crystals of the LILRB1-pHLA-A2 complexes appeared after 1–2 weeks at 23 °C (Table 1).

Prior to X-ray data collection LILRB1-pHLA-A2 complex crystals were soaked in reservoir solution incorporating increasing concentrations of ethylene glycol (18–22%) and flash cooled in liquid nitrogen. X-ray diffraction data for the LILRB1-HLA-A2<sup>ILKEPVHGV</sup> complex were collected to 2.4 Å resolution with the ADSC Quantum 4 detector at beamline ID14–4 (ESRF). The LILRB1-HLA-A2<sup>ILKEPVHGV</sup> complex crystallised in the trigonal space group  $P3_221$ , with two molecules per asymmetric unit, and unit cell parameters  $a = b = 116.2$  Å and  $c = 192.8$  Å. For all other LILRB1-pHLA-A2 complexes, X-ray data were collected with an ‘in-house’ MicroMax 007HF rotating anode Rigaku X-ray generator using a Saturn 944 CCD detector. The LILRB1-pHLA-A2 complex typically crystallizes in the trigonal space group  $P3_221$ , with 2 molecules per asymmetric unit. All data were processed using the XDS suite (Kabsch, 2010) and the relevant statistics are listed in Table 2.

### 2.3 Structure determination and refinement

The 2.4 Å resolution LILRB1-HLA-A2<sup>ILKEPVHGV</sup> complex structure was solved by molecular replacement using MOLREP (Vagin and Teplyakov, 2010). The search model consisted of the LILRB1-HLAA2<sup>ILKEPVHGV</sup> complex refined to 3.4 Å resolution ((Willcox et al., 2003); PDB code 1P7Q). The LILRB1-HLA-A2<sup>RQASIELPSMAV</sup>, LILRB1-HLAA2<sup>RTFSPTYGL</sup> and LILRB1-HLA-A2<sup>RLSSPLHFV</sup> complex structures were also determined by molecular replacement using the high-resolution LILRB1-HLA-A2<sup>ILKEPVHGV</sup> structure complex as the search model with the co-ordinates of the ILK peptide moiety omitted. The structures were refined by alternating cycles of energy-minimization and B-factor refinement using CNS and REFMAC5 (Brunger et al., 1998; Murshudov et al., 2011). Manual rebuilding was performed with the graphics program COOT (Emsley et al., 2010). All of the complexes demonstrated unequivocal  $F_o - F_c$  difference density for the epitopes, which were directly built into each of the structures. The stereochemical and refinement parameters are listed in Table 2. Structure validation and analysis were carried out with CCP4 suite (Winn et al., 2011). The atomic coordinates and structure factors have been deposited in the RCSB Protein Data Bank. Figures were generated using the programs POVSCRIPT (Fenn et al., 2003), Pov-Ray (<http://www.povray.org>) and PyMOL (Schrodinger, 2015).

Table 2 Data processing and refinement statistics for the LILRB1-HLA-A2<sup>ILKEPVHGV</sup>, LILRB1-HLA-A2<sup>RTFSPTYGL</sup> and LILRB1-HLA-A2<sup>RLSSPLHYV</sup> complex structures. Figures in parentheses in the data processing section apply to data in the highest resolution shell.

	<b>LILRB1-HLAA2-ILK</b>	<b>LILRB1-HLAA2-RTFS</b>	<b>LILRB1-HLA-A2-RLSS</b>
PDB ID code	6EWA	6EWO	6EWC
Peptide sequence	ILKEPVHGV	RTFSPTYGL	RLSSPLHYV
Data processing			
Resolution (Å)	48.6–2.4 (2.5–2.4)	20–2.3 (2.4–2.3)	20–3.2 (3.1–3.2)
Unit cell dimensions (Å)	116.1, 116.1, 192.8	116.3, 116.3, 192.6	117.5, 117.5, 203.7
Space Group	P3221	P3221	P3221
Total reflections	578,024 (80872)	758,810 (41698)	149,740 (12971)
Unique reflections	60,013 (8505)	66,969 (7259)	26,415 (2338)
Multiplicity	9.6 (9.5)	11.3 (5.5)	5.7 (5.5)
Completeness (%) <sup>a</sup>	99.6 (99.7)	99.1 (94)	96 (98.6)
R <sub>merge</sub> (%) <sup>b</sup>	12.2 (53.7)	10 (73.4)	17.3 (44.2)
I/σ(I)	5.2 (1.4)	23.6 (2.8)	10.7 (3.9)
Refinement			
Resolution (Å)	48.6–2.4	19.7–2.3	19.58–3.2
Reflections used	56,939	63,567	26,414
R <sub>cryst</sub> (%) <sup>c</sup>	22.8	23.4	20.6
R <sub>free</sub> (%) <sup>d</sup>	27.9	27.6	24.5
Protein residues	1101	1117	1122
Water molecules	45	228	–
Model geometry			
Ramachandran plot			
Most favoured	90.8	89	88.5
Additionally allowed	8.1	9.6	10.1
Generously allowed	0.7	1.0	0.9
Disallowed	0.4	0.4	0.5
RMS deviations			
Bond lengths (Å)	0.008	0.008	0.008
Bond angles (°)	1.26	1.29	1.19

### 3. Results.

#### 3.1 HIL-A1 bound phosphopeptides can be refractory to crystallisation

During our previous studies of phosphopeptide presentation by HLA-A2 we found that, whereas canonical P4-phosphorylated phosphopeptides were amenable to crystallisation, the majority of their unmodified counterparts, with the exception of a few isolated examples (Mohammed et al., 2017, Petersen et al., 2009), proved highly intransigent to crystallisation. Similarly, structural determination of pMHC in complex with “non-canonical” (i.e. non-P4 phosphorylated)

phosphopeptides was also hampered by the majority of such complexes being refractory to crystallisation (Table 1). Hence our attempts at structure determinations of both non-phosphorylated pMHC and noncanonical phosphopeptide antigens highlighted the need for an alternative strategy to aid pMHC crystallisation.

### 3.2. Validating the LILRB1 strategy for crystallising intransigent HLA-A2 molecules

We explored the possibility of co-crystallising intransigent pMHC complexes with a natural immune receptor ligand. One candidate receptor that reproducibly co-crystallizes with HLA-A2 is LILRB1, which binds to the non-polymorphic regions of the MHC protein comprised of the  $\alpha 3$  and  $\beta 2M$  domains. Crucially, the LILRB1-pMHC interface is located distally to the peptide-binding site (Willcox et al., 2003), suggesting that it is highly unlikely to interfere with epitope conformation. Comparison of the LILRB1-HLA-A2<sup>ILKEPVHGV</sup> complex (Willcox et al., 2003) with previous structural analyses of HLA-A2<sup>ILKEPVHGV</sup> (Madden et al., 1993) failed to note any differences in the HLA-A2 bound peptide in the presence/absence of LILRB1 (Willcox et al., 2003). However, LILRB1-HLA-A2<sup>ILKEPVHGV</sup> structural data were only available to 3.4 Å, limiting detailed analysis of the peptide conformation. To definitively resolve whether the binding of LILRB1 to HLA-A2 affected peptide conformation, we determined a higher resolution structure of the LILRB1-HLA-A2<sup>ILKEPVHGV</sup> complex (to 2.4 Å resolution (Fig. 1a)), which enabled a more accurate structure of the ILK peptide moiety (Fig. 1b). Structural overlay comparisons of this higher resolution LILRB1-HLA-A2 structure with the HLA-A2<sup>ILKEPVHGV</sup> determined in the absence of LILRB1 (Madden et al., 1993) demonstrated that the peptide binding platform in both complexes was very similar with an r.m.s.d value of 0.6 Å (Fig. 1c). Most crucially, no significant changes in structure of the ILK peptide epitope were evident upon LILRB1 binding to HLA-A2 as demonstrated by the low r.m.s.d value of 0.24 Å (Fig. 1d). This confirmed that co-crystallisation of LILRB1 with HLA-A2 complex does not alter the conformation of the MHC-bound antigenic peptide, and established a basis for exploring its potential as a chaperone for facilitating crystallisation of pMHC complex molecules.

### 3.3. LILRB1 facilitates crystallisation and structure determination of tumour-associated pHLA-A2-complexes

To assess whether LILRB1 could promote the crystallisation of pMHC complexes, we selected several pHLA-A2 complexes that had previously proven to be refractory to crystallisation, based on extensive nanolitre-scale crystallisation trials using commercial screening kits, at concentrations commonly used for class I MHC crystallisation (typically 10–25 mg/ml). These were generally tumour associated phosphopeptides, and their unphosphorylated counterparts (Zarling et al., 2006). LILRB1 and pHLA-A2 complexes were produced as previously described (Willcox et al., 2003).

Initial attempts at crystallising pMHC complexes previously found to be refractory to crystallisation alone, frequently resulted in multiple hits in co-crystallisation trials with LILRB1 (Table 1). Initial attempts focussed on non-phosphorylated antigens, which involved equilibrating against conditions that had yielded LILRB1-HLA-A2<sup>ILKEPVHGV</sup> crystals, revealed a crystallisation solution (PEG 3350, Ammonium acetate and, Tris-HCl – hereafter referred to as PAT) that proved somewhat generic, as it was successful in providing useful primary hits for a diverse subset of pMHC complexes previously intransigent to crystallisation. An example included the 10-mer HLA-A2<sup>KMDSFLDMQL</sup> peptide complex, crystals of which grew with a morphology similar to that of LILRB1-HLA-A2<sup>ILKEPVHGV</sup> crystals (Fig. 2a), in the presence of LILRB1. In addition, the 12-mer HLA-A2<sup>RQASIELPSMAV</sup> complex also previously intransigent to crystallisation, yielded crystals with LILRB1 that grew in an optimised form of the generic PAT crystallisation reagent (comprised of 20% PEG 3350, 0.2 M ammonium acetate and 0.1 M HEPES pH 7.4 – hereafter referred to as PAH) (Fig. 2b). Crucially, this same PAH condition failed to crystallise HLA-A2<sup>RQASIELPSMAV</sup> in the absence of LILRB1, underlining the critical chaperone function of

LILRB1 in the crystallisation process. Importantly, the PAT condition also demonstrated considerable promise for crystallising HLA-A2 molecules bound to non-canonical phosphopeptides, including the 9-mer (IMDRpTPEKL) (Fig. 2c) and 11-mer (KLIDIVpSSQKV) (Fig. 2d).

Despite successful use of the PAT condition as a generic crystallisation condition for a subset of peptide-HLA-A2 complexes, for other peptide-HLA-A2 complexes fresh crystallisation hits were identified in the presence of LILRB1 following rescreeing of complexes against commercial sparse matrix kits. An example was HLA-A2<sup>RTFSPTYGL</sup>, which yielded co-crystals with LILRB1 from the PEG Ion screen in the presence of 0.2 M potassium sodium tartrate and 20% PEG 3350 (Fig. 2e). A similar LILRB1 co-crystallisation screening strategy for the HLA-A2<sup>RLSSPLHFV</sup> complex resulted in initial micro-crystals obtained in drops equilibrated against 3% Tacsimate pH 6 and 12.8% PEG 3350, after which further optimisations in the presence of dimethyl sulphoxide produced large well ordered LILRB1-HLA-A2<sup>RLSSPLHFV</sup> complex crystals (Fig. 2f). Finally, it was possible to crystallise the HLA-A2RLQSTSERL complex, which we found previously was intransigent to crystallisation attempts, in complex with LILRB1 in the presence of 0.2 M Potassium Acetate and 20% PEG 3350, resulting in microcrystals worthy of further optimisation (Fig. 2g).

When combining the two groups of antigens we focussed on (nonphosphorylated counterparts of P4 phosphopeptides, and non-canonical phosphopeptides), only 10 out of the 19 pMHC complexes yielded hits with conventional trials (Table 1). In contrast, a majority of pMHC complexes (8/9) generated hits when co-crystallised with LILRB1 (Table 1). Furthermore, several complexes yielded multiple independent hits thereby increasing the likelihood of growing diffraction-grade crystals (> 5, Table 1).

Crystals produced using the LILRB1 co-crystallisation strategy were of sufficient quality for data collection. Optimised LILRB1 co-crystals of the unmodified 12-mer, LILRB1-HLA-A2<sup>ROASIELPSMAV</sup> complex (Fig. 2d), permitted data collection and structure determination to 2.7 Å (Mohammed et al., 2017). Moreover, LILRB1 co-crystals of the HLA-A2<sup>RTFSPTYGL</sup> and HLA-A2<sup>RLSSPLHFV</sup> complexes diffracted X-rays to 2.3 Å and 3.2 Å, resulting in full structure determinations (Fig. 3). The quality of the resulting electron density maps were significantly improved using two-fold non-crystallographic symmetry averaging, which is present in all LILRB1-pHLA-A2 complex crystals, thereby aiding model building and structure determination (Fig. 3, Table 2). Collectively, these results clearly highlight the potential of exploiting LILRB1 as a crystallisation chaperone, to facilitate X-ray crystallographic analyses of biologically important peptide-HLA-A2 complexes.

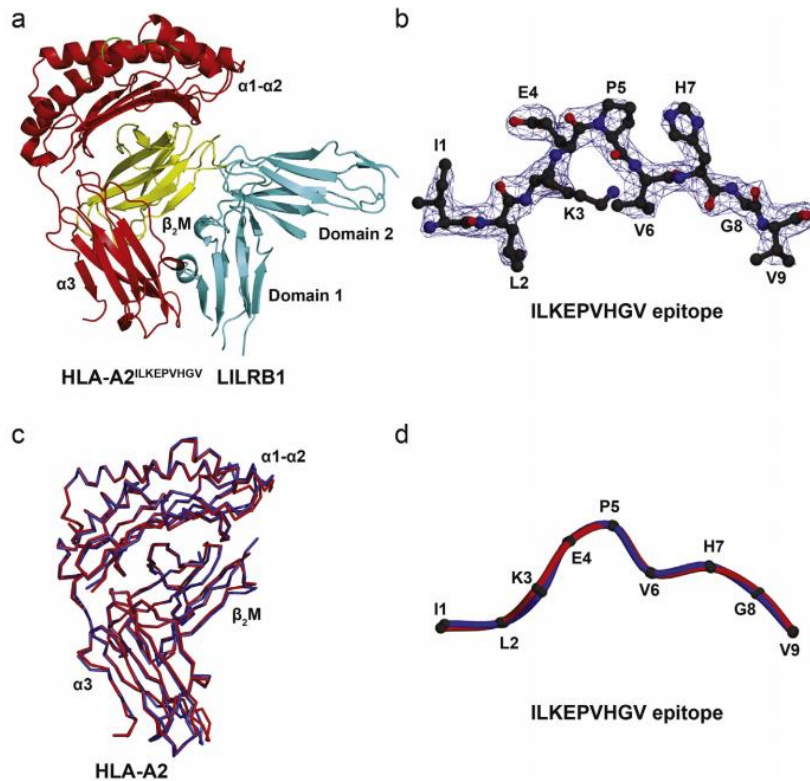


Figure 1 Co-crystallisation of LILRB1 with HLA-A2 does not alter the conformation of the MHC-bound antigenic peptide. (a) Ribbon representation of the LILRB1-HLA-A2<sup>ILKEPVHGV</sup> complex structure determined to 2.4 Å resolution (HLA-A2 α chain (red), β<sub>2</sub>-microglobulin (yellow) and LILRB1 (cyan)). (b) 2*Fo*-*Fc* electron density map contoured at 1.0 σ (blue wire) for the ILK peptide moiety bound within the HLA-A2 peptide binding cleft. (c) Superimposition of the HLA-A2 C-α chains determined in the presence (red) and absence (blue) of LILRB1. The co-ordinates for the HLA-A2<sup>ILKEPVHGV</sup> complex were retrieved from the PDB (accession code (1HHJ)) (Madden et al., 1993). (d) Overlay of the ILK peptide moiety derived from HLA-A2 in the presence (red) and absence (blue) of LILRB1. (For interpretation of the references to colour in this figure legend, the reader is referred to the web version of this article.)

### 3.4. LILRB1/HLA-A2 crystal contacts are conserved for other pMHC molecules

To assess the possibility that this approach might also be relevant for improving crystallisation of other MHC molecules known to bind LILRB1 (Chapman et al., 1999), we first aligned the sequences of HLA-A2, HLA-B27, HLA-Cw06, HLA-E, HLA-F and HLA-G1 using PRALINE (Fig. 4a). Analysis of HLA-A2 heavy chain crystal contacts in our LILRB1-HLA-A2 complex structures highlighted that of the total 84 residues forming crystal contacts (Fig. 4b), 44 are conserved across class I MHC, 33 are semi-conserved and 5 are non-conserved (Fig. 4a). This demonstrates that the majority of HLA-A2 residues involved in forming crystal contacts within LILRB1/HLA-A2 crystals are conserved in many different class I MHC molecules.

## 4. Discussion.

Structural studies of class I peptide MHC structures continue to make major contributions to our understanding of important areas of immunobiology. However, despite availability of numerous pMHC structures, reliable structural analyses of predefined pMHC targets can still be challenging, as certain pMHC complexes can be intractable to crystallisation. This represents a significant impediment to molecular studies aiming to define the role of MHC-restricted antigenic peptide epitopes in specific immunobiological contexts such as disease pathogenesis and immunotherapeutic development. In the context of MHC alleles that have been crystallised, this phenomenon is superficially surprising, given conservation of the alpha chain and β<sub>2</sub>M, and the fact

that only the peptide moiety would be altered between each individual pMHC complex. Whilst the molecular basis underlying it is unclear, it is likely to result from the hugely diverse properties of bound peptides. Given the strong link between protein stability and propensity for crystallisation, one significant factor is likely to be the wide span of peptide binding affinities for MHC, and the relative kinetics of complex dissociation and aggregation, versus crystal nucleation. However, our demonstration that peptides with similar epitope sequence and binding affinities, such as RQA\_V in its phosphorylated and non-phosphorylated states (Mohammed et al., 2017), may not exhibit the same propensity for crystallisation, suggests that factors other than peptide affinity, such as the potential of peptide conformation to favour or disrupt crystal packing interactions, or differential complex solubility, are likely to be relevant to crystal formation.

In this study we investigated a novel strategy for circumnavigating crystallisation of intransigent pMHC complexes. The approach relies upon the addition of a natural ligand of class I MHC, LILRB1, to promote alternative, and in many cases more optimal crystal packing contacts. Our findings, focused in this study on the HLA-A2 allele, highlight that LILRB1 can serve as an effective non-covalent crystallisation chaperone for peptide-HLA-A2 complexes. This strategy offers several advantages. Firstly, since co-crystallisation with LILRB1 does not perturb the biologically critical  $\alpha 1\alpha 2$  peptide-binding platform, it allows bone fide peptide conformation to be observed. Secondly, the approach is experimentally highly feasible. LILRB1 is easily over-expressed in large amounts into *E. coli* inclusion bodies (typical yields of 100 g/l), and renaturation and purification is relatively efficient. Moreover, peptide-HLA-A2 crystallisation optimisation with LILRB1, which exploits a generic crystallisation condition in many cases, is extremely efficient, and results in the production of large crystals within a relatively short time interval (< 2 weeks), often of a sufficient size for data collection. Although we did not formally prove that all such crystals were of LILRB1-HLA-A2 complex, single protein controls (HLAA2 or LILRB1 alone) did not yield crystals under similar conditions. Furthermore, both the timescale of crystallisation, the crystal morphology and when x-ray data were collected the trigonal space group and unit cell constants were all characteristic of LILRB1-HLA-A2 complex crystals. Moreover, while such crystals yield acceptable data using 'in-house' sources, clearly use of synchrotron sources would inevitably improve resolution further. In addition, the availability of the higher resolution structure of LILRB1 provides useful model-based phase information necessary for resolving LILRB1-pHLA-A2 complexes, a process that has become increasingly routine since all LILRB1-pHLA-A2 crystals exhibit similar unit cell constants, even if grown in chemically distinct conditions. Typically, the presence of two LILRB1-HLA-A2-peptide complexes in the asymmetric unit allows non-crystallographic symmetry averaging, improving the quality of the electron density. Thirdly, based on the evidence we present here, LILRB1 co-crystallisation is clearly an approach capable of catalyzing crystallisation of a diverse range of peptides in the context of HLA-A2, including those previously intransigent to crystallisation.

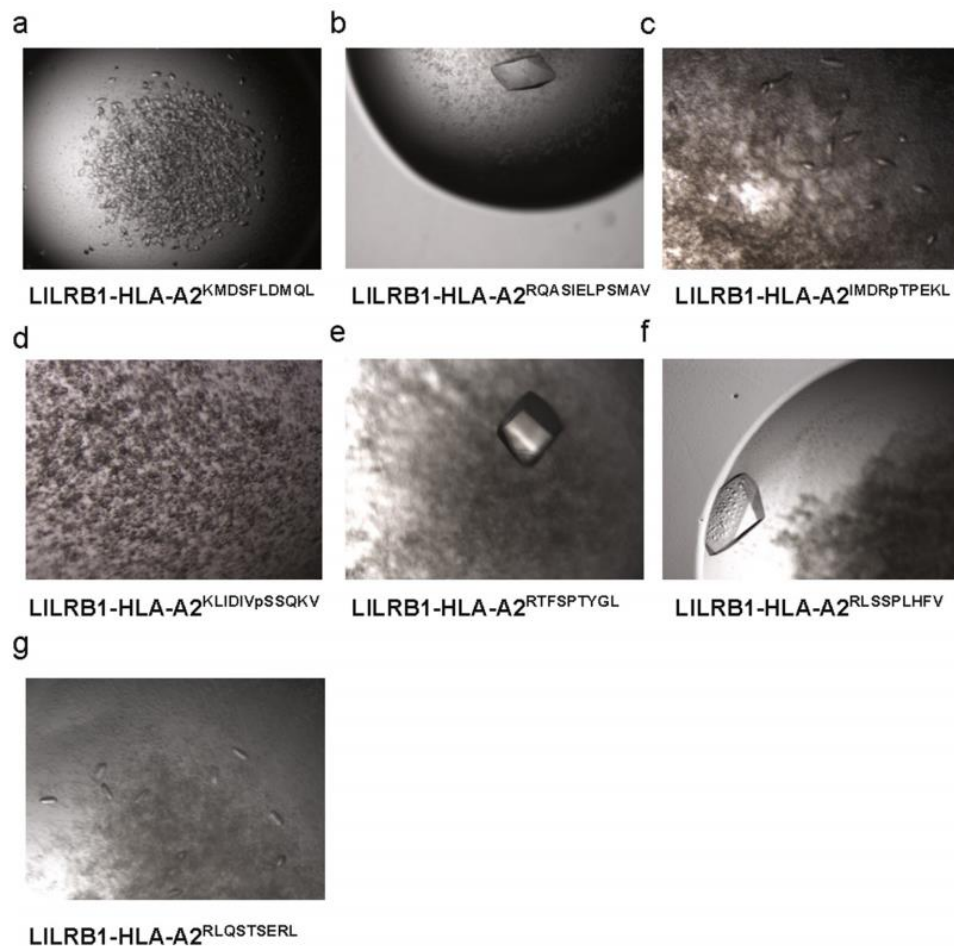


Figure 2 Crystallisation of intrinsigent HLA-A2-peptide complexes with LILRB1. Crystal morphologies of LILRB1-HLA-A2<sup>KMDSFQDMQL</sup> (a), LILRB1-HLA-A2<sup>RQASIELPSMAV</sup> (b), LILRB1-HLA-A2<sup>IMDRpTPEKL</sup> (c), LILRB1-HLA-A2<sup>KLIDIVpSSQKV</sup> (d), LILRB1-HLA-A2<sup>RTFSPTYGL</sup> (e), LILRB1-HLA-A2<sup>RLSSPLHFV</sup> (f) and LILRB1-HLA-A2<sup>RLQSTSERL</sup> (g).

Two observations highlight that the LILRB1 chaperone approach we outline here might be applicable to different class I MHC molecules. Firstly, LILRB1 is known to recognize a broad range of class I pMHC molecules, which is explained by its recognition of a relatively nonpolymorphic region of the class I MHC molecule (the  $\alpha 3$  domain, as well as  $\beta 2$ -microglobulin) that is substantially conserved across different of different classical (HLA-A, -B, -C) and non-classical (HLA-E, -F, -G) molecules. Secondly, a majority of HLA-A2 residues involved in forming crystal contacts within LILRB1-HLA-A2 crystals are conserved in a diverse range of classical/non-classical class I MHC molecules. Therefore there is considerable potential for extending the current strategy to facilitate crystallisation of a more diverse range of class I MHC molecules, although this is a focus for future studies.

Development of LILRB1 as a crystallisation chaperone for pMHC could have several applications. Immune presentation and recognition of post-translationally modified peptide antigens is increasingly recognised as an area of immunobiological importance, not least in the context of cancer immunosurveillance and immunotherapy. We have successfully applied the method to dissect the effects of phosphorylation on peptide conformation. Of relevance in this context, so-called “non-canonical” phosphopeptide HLA-A2 complexes, for which limited structural data are available, have proven to be relatively intrinsigent to conventional crystallisation attempts; furthermore unmodified counterparts of naturally occurring phosphopeptides tend to be notably lower affinity, and would be expected to represent challenging crystallisation targets. Use of LILRB1 as a crystallisation chaperone facilitated crystallisation of several such peptides. In addition, the

method may also be particularly suitable for longer, more bulged peptides (either unmodified or those bearing bulky post-translational modifications), where conventional class I MHC crystal packing interactions may be disrupted. Of relevance to this grouping, exhaustive conventional attempts to crystallise the bulky 12-mer unmodified HLA-A2<sup>RQASIELPSMAV</sup> complex failed entirely, despite in this case an equivalent affinity to the naturally phosphorylated form. The LILRB1 chaperone approach quickly led to its structure determination, allowing us to demonstrate that phosphorylation of this leukaemia-associated epitope resulted in an unprecedented conformational change relative to this unmodified form, creating a highly distinct conformational “neoepitope” (Mohammed et al., 2017). Indeed, examination of the structure of unphosphorylated HLA-A2<sup>RQASIELPSMAV</sup> in complex with LILRB1 provided a molecular explanation for its failure to crystallise alone, highlighting a more pronounced bulge to the peptide conformation at P8 (Proline) that precluded crystallisation in the same mode as the phosphorylated form (HLA-A2<sup>RQApSIELPSMAV</sup>) by causing steric clashes with a neighbouring molecule. This observation highlights that altered crystal contacts introduced by LILRB1 co-crystallisation can clearly circumvent such problems. A second scenario, peptide anchor modification, which is an immunotherapeutic approach used to boost antigen immunogenicity whereby peptide immunogens are engineered with modified anchor residues to optimise MHC binding, is another setting where the LILRB1 crystallisation chaperone methodology could be productively applied. Here the intention is to increase MHC affinity but without altering peptide conformation presented to TCR. Structural comparisons of unmodified and modified forms (the former by definition of low affinity) are likely to be highly informative in this setting. In addition, there has been considerable interest in the potential to crystallise ‘empty’ class I MHC molecules that lack bound peptide, and this would be another worthy application of the LILRB1 crystallisation chaperone approach.

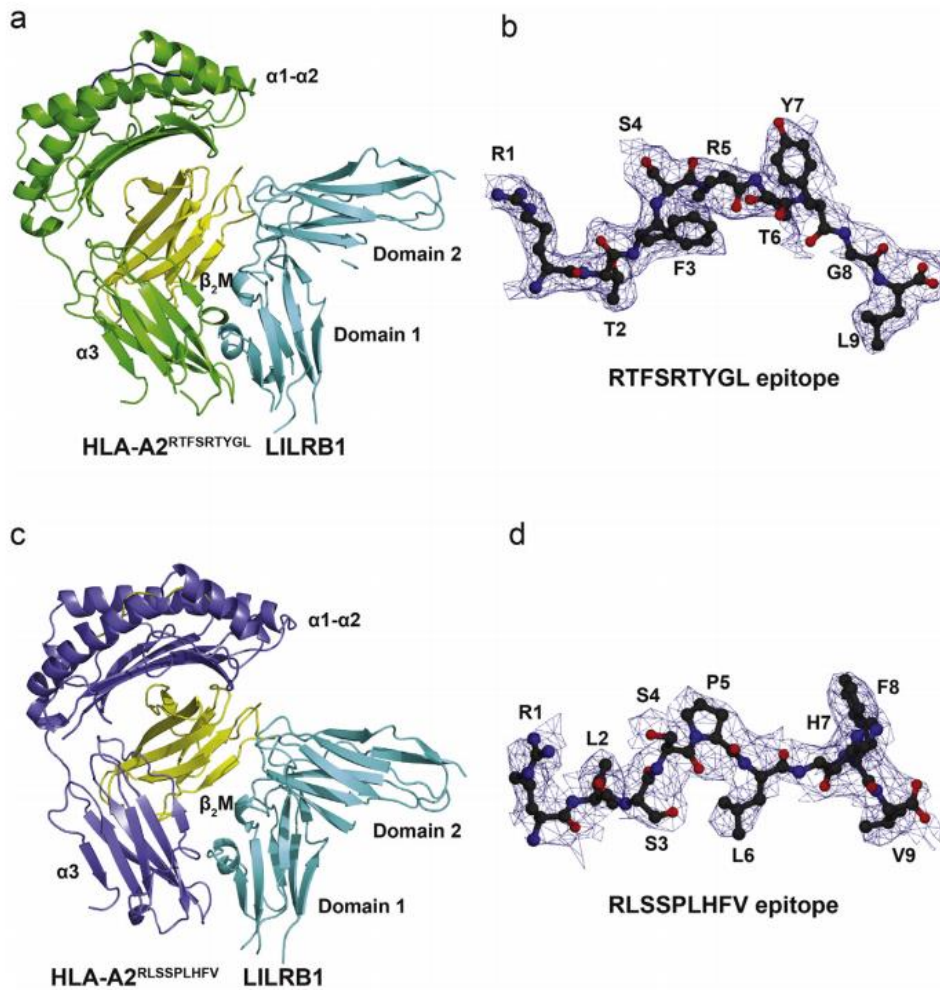


Figure 3 Crystal structures of LILRB1-HLA-A2<sup>RTFSPTYGL</sup> and LILRB1-HLA-A2<sup>RLSSPLHFV</sup> complexes. (a) Ribbon representation of the LILRB1-HLA-A2<sup>RTFSPTYGL</sup> complex structure determined to 2.3 Å resolution (HLAA2  $\alpha$  chain (green),  $\beta_2$ -microglobulin (yellow) and LILRB1 (cyan)). (b) 2Fo-Fc electron density map contoured at 1.0  $\sigma$  (blue wire) for the RTF peptide moiety bound within the HLA-A2 peptide binding groove. (c) Ribbon representation of the LILRB1- HLA-A2<sup>RLSSPLHFV</sup> complex structure determined to 3.2 Å resolution (HLA-A2  $\alpha$  chain (purple),  $\beta_2$ -microglobulin (yellow) and LILRB1 (cyan)). (d) 2Fo-Fc electron density map contoured at 1.0  $\sigma$  (blue wire) for the RLS peptide moiety bound within the HLA-A2 peptide binding cleft. (For interpretation of the references to colour in this figure legend, the reader is referred to the web version of this article.)

In light of our results, we propose that other class I MHC receptors could be exploited as alternative crystallisation chaperones - for class I pMHC, the two most likely candidates are LILRB2 and CD8 $\alpha$ , both of which bind to a broad range of class I MHC molecules (Chapman et al., 1999; Gao et al., 2000). Moreover, previous structural studies of both LILRB2 and CD8 $\alpha$  immune receptors in complex with class I MHC have highlighted that they interact with sites of the MHC that are distal to the antigen binding platform and therefore are highly unlikely to influence epitope conformation (Gao et al., 1997; Shiroishi et al., 2006). LILRB2 displays an overlapping but distinct MHC-I recognition mode relative to LILRB1 and predominantly mediates hydrophobic contacts to the HLA-G  $\alpha 3$  domain (Shiroishi et al., 2006). Moreover, structural comparisons of HLA-G and its bound peptide in the presence and absence (Clements et al., 2005) of LILRB2 have demonstrated no substantial shifts in conformation (Fig. 5a–b) thus confirming the potential of LILRB2 as a tool for promoting protein crystallisation of nonclassical MHC molecules. In contrast, the CD8 $\alpha$ -MHC binding interaction mode significantly differs to that of LILRB1 and LILRB2 forming interactions with the  $\alpha 2$  and  $\alpha 3$  domains of HLA-A2 as well as  $\beta_2 M$  (Gao et al., 1997), but similarly has no significant effects on the conformation of the  $\alpha 1\alpha 2$  peptide binding platform (Fig. 5c–d). Therefore LILRB2 and CD8 $\alpha$



representation of HLA-A2 heavy chain derived from HLA-A2-LILRB1 complex structure (green). For clarity the LILRB1 and  $\beta_2M$  molecules have been omitted. HLA-A2 alpha chain residues that contribute to crystal contacts have been mapped (pink spheres). (For interpretation of the references to colour in this figure legend, the reader is referred to the web version of this article.)

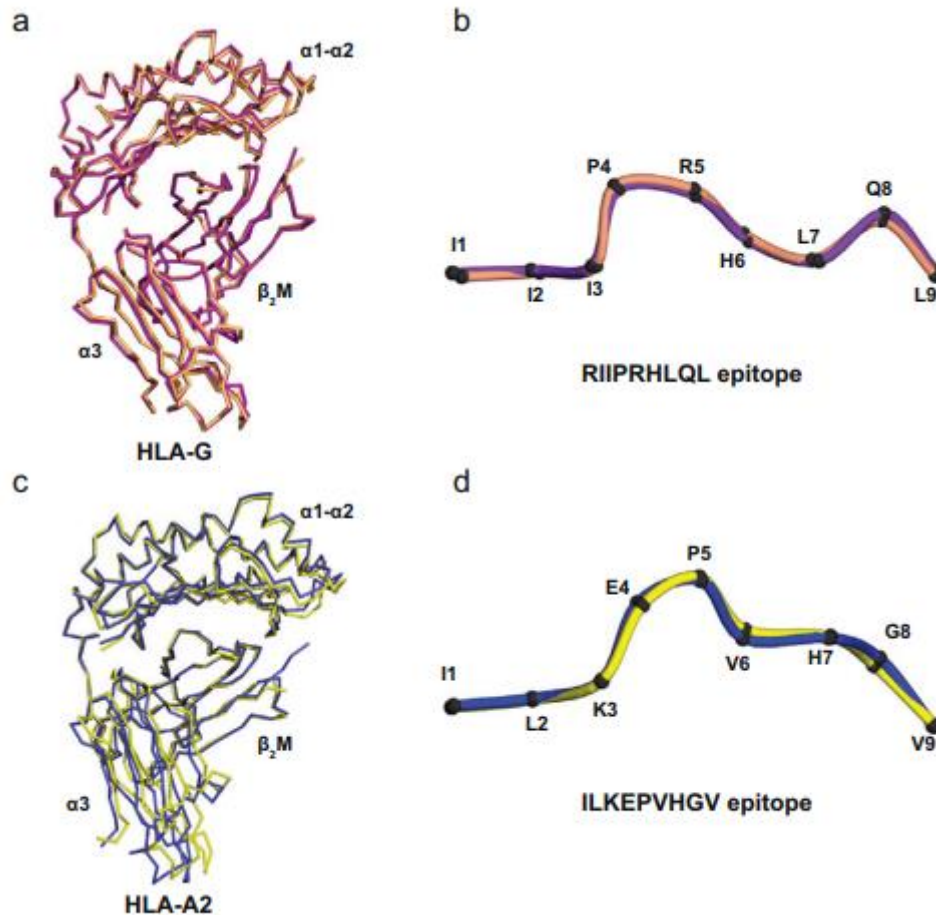


Figure 5 Co-crystallisation of LILRB2 or CD8 $\alpha$  with MHC class I molecules does not affect the conformation of the bound antigenic peptide. (a) Superimposition of the HLA-G C- $\alpha$  chains determined in the presence (purple) and absence (pink) of LILRB2. The co-ordinates were retrieved from the PDB (accession codes for HLA-G<sup>RIIPRHLQL</sup> (1YDP) (Clements et al., 2005) and HLA-G<sup>RIIPRHLQL</sup>-LILRB2 (2DYP) (Shiroishi et al., 2006) (b) Overlay of the RII peptide moiety derived from HLA-G in the presence (purple) and absence (pink) of LILRB2. (c) Superimposition of the HLA-A2 C- $\alpha$  chains determined in the presence (yellow) and absence (blue) of CD8 $\alpha$ . The co-ordinates were retrieved from the PDB (accession codes for HLA-A2<sup>ILKEPVHGV</sup> (1HHJ)(Madden et al., 1993) and HLAA2ILKEPVHGV-CD8 $\alpha$  (1AKJ) (Gao et al., 1997)(d) Overlay of the ILK peptide moiety derived from HLA-A2 in the presence (yellow) and absence (blue) of CD8 $\alpha$ . (For interpretation of the references to colour in this figure legend, the reader is referred to the web version of this article.)

## Conflict of interest

The authors declare that they have no conflicts of interest with the contents of this article.

## Author contributions

FM and DHS designed the study and carried out experiments. FM and DHS analysed data and wrote the manuscript. BEW designed the study, analysed data and wrote the manuscript.

## Acknowledgements

We acknowledge the Birmingham Protein Expression Facility for assistance with recombinant protein production. This work was funded by a Wellcome Trust New Investigator Award (Grant reference number: 099266/Z/12/Z). DHS was supported by a Medical Research Council studentship.

## Appendix A. Supplementary data

Supplementary data to this article can be found online at [insert official URL]

## References

Bjorkman, P.J., Saper, M.A., Samraoui, B., Bennett, W.S., Strominger, J.L., Wiley, D.C., 1987. Structure of the human class I histocompatibility antigen, HLA-A2. *Nature* 329, 506–512.

Brunger, A.T., Adams, P.D., Clore, G.M., Delano, W.L., Gros, P., Grosse-Kunstleve, R.W., Jiang, J.-S., Kuszewski, J., Nilges, M., Pannu, N.S., Read, R.J., Rice, L.M., Simonson, T., Warren, G.L., 1998. Crystallography & NMR system: a new software suite for macromolecular structure determination. *Acta Crystallogr. Sect. D* 54, 905–921.

Bukowska, M.A., Grütter, M.G., 2013. New concepts and aids to facilitate crystallization. *Curr. Opin. Struct. Biol.* 23, 409–416.

Bulek, A.M., Madura, F., Fuller, A., Holland, C.J., Schauenburg, A.J.A., Sewell, A.K., Rizkallah, P.J., Cole, D.K., 2012. TCR/pMHC optimized protein crystallization screen. *J. Immunol. Methods* 382, 203–210.

Chapman, T.L., Heikema, A.P., Bjorkman, P.J., 1999. The inhibitory receptor LIR-1 uses a common binding interaction to recognize class I MHC molecules and the viral homolog UL18. *Immunity* 11, 603–613.

Clements, C.S., Kjer-Nielsen, L., Kostenko, L., Hoare, H.L., Dunstone, M.A., Moses, E., Freed, K., Brooks, A.G., Rossjohn, J., McCluskey, J., 2005. Crystal structure of HLA-G: a nonclassical MHC class I molecule expressed at the fetal–maternal interface. *Proc. Natl. Acad. Sci. U. S. A.* 102, 3360–3365.

Cobbold, M., De La Peña, H., Norris, A., Polefrone, J.M., Qian, J., English, A.M., Cummings, K.L., Penny, S., Turner, J.E., Cottine, J., Abelin, J.G., Malaker, S.A., Zarlign, A.L., Huang, H.-W., Goodyear, O., Freeman, S.D., Shabanowitz, J., Pratt, G., Craddock, C., Williams, M.E., Hunt, D.F., Engelhard, V.H., 2013. MHC class I-associated phosphopeptides are the targets of memory-like immunity in leukemia. *Sci. Transl. Med.* 5 (203ra125-203ra125).

Depontieu, F.R., Qian, J., Zarlign, A.L., McMiller, T.L., Salay, T.M., Norris, A., English, A.M., Shabanowitz, J., Engelhard, V.H., Hunt, D.F., Topalian, S.L., 2009. Identification of tumor-associated, MHC class II-restricted phosphopeptides as targets for immunotherapy. *Proc. Natl. Acad. Sci. U. S. A.* 106, 12073–12078.

Derewenda, Z.S., 2010. Application of protein engineering to enhance crystallizability and improve crystal properties. *Acta Crystallogr. D Biol. Crystallogr.* 66, 604–615.

Dulberger, C.L., McMurtrey, C.P., Hölzemer, A., Neu, K.E., Liu, V., Steinbach, A.M., Garcia-Beltran, W.F., Sulak, M., Jabri, B., Lynch, V.J., Altfeld, M., Hildebrand, W.H., Adams, E.J., 2017. Human Leukocyte Antigen F Presents Peptides and Regulates Immunity through Interactions with NK Cell Receptors. *Immunity* 46 (1018–1029.e1017).

- Emsley, P., Lohkamp, B., Scott, W.G., Cowtan, K., 2010. Features and development of coot. *Acta Crystallogr. D Biol. Crystallogr.* 66, 486–501.
- Fenn, T.D., Ringe, D., Petsko, G.A., 2003. POVScript+: a program for model and data visualization using persistence of vision ray-tracing. *J. Appl. Crystallogr.* 36, 944–947.
- Gao, G.F., Tormo, J., Gerth, U.C., Wyer, J.R., McMichael, A.J., Stuart, D.I., Bell, J.I., Jones, E.Y., Jakobsen, B.K., 1997. Nature 387, 630–634 Crystal structure of the complex between human CD8[alpha][alpha] and HLA-A2.
- Gao, G.F., Willcox, B.E., Wyer, J.R., Boulter, J.M., O'Callaghan, C.A., Maenaka, K., Stuart, D.I., Jones, E.Y., Van Der Merwe, P.A., Bell, J.I., Jakobsen, B.K., 2000. Classical and nonclassical class I major histocompatibility complex molecules exhibit subtle conformational differences that affect binding to CD8 $\alpha\alpha$ . *J. Biol. Chem.* 275, 15232–15238.
- Garboczi, D.N., Hung, D.T., Wiley, D.C., 1992. HLA-A2-peptide complexes: refolding and crystallization of molecules expressed in *Escherichia coli* and complexed with single antigenic peptides. *Proc. Natl. Acad. Sci. U. S. A.* 89, 3429–3433.
- Griffin, L., Lawson, A., 2011. Antibody fragments as tools in crystallography. *Clin. Exp. Immunol.* 165, 285–291.
- Hoppes, R., Oostvogels, R., Luimstra, J.J., Wals, K., Toebes, M., Bies, L., Ekkebus, R., Rijal, P., Celie, P.H.N., Huang, J.H., Emmelot, M.E., Spaapen, R.M., Lokhorst, H., Schumacher, T.N.M., Mutis, T., Rodenko, B., Ovaa, H., 2014. Altered peptide ligands revisited: vaccine design through chemically modified HLA-A2–restricted T cell epitopes. *J. Immunol.* 193, 4803.
- Illing, P.T., Vivian, J.P., Dudek, N.L., Kostenko, L., Chen, Z., Bharadwaj, M., Miles, J.J., Kjer-Nielsen, L., Gras, S., Williamson, N.A., Burrows, S.R., Purcell, A.W., Rossjohn, J., McCluskey, J., 2012. Immune self-reactivity triggered by drug-modified HLA-peptide repertoire. *Nature* 486, 554–558.
- Jones, D.C., Kosmoliaptsis, V., Apps, R., Lapaque, N., Smith, I., Kono, A., Chang, C., Boyle, L.H., Taylor, C.J., Trowsdale, J., Allen, R.L., 2011. HLA class I allelic sequence and conformation regulate leukocyte Ig-like receptor binding. *J. Immunol.* 186, 2990–2997.
- Kabsch, W., 2010. XDS. *Acta Crystallogr. D* 66, 125–132.
- Madden, D.R., 1995. The three-dimensional structure of peptide-MHC complexes. *Annu. Rev. Immunol.* 13, 587–622.
- Madden, D.R., Garboczi, D.N., Wiley, D.C., 1993. The antigenic identity of peptide-MHC complexes: a comparison of the conformations of five viral peptides presented by HLA-A2. *Cell* 75, 693–708.
- Madura, F., Rizkallah, P.J., Holland, C.J., Fuller, A., Bulek, A., Godkin, A.J., Schauenburg, A.J., Cole, D.K., Sewell, A.K., 2015. Structural basis for ineffective T-cell responses to MHC anchor residue-improved “heteroclitic” peptides. *Eur. J. Immunol.* 45, 584–591.
- Mohammed, F., Cobbold, M., Zarling, A.L., Salim, M., Barrett-Wilt, G.A., Shabanowitz, J., Hunt, D.F., Engelhard, V.H., Willcox, B.E., 2008. Phosphorylation-dependent interaction between antigenic peptides and MHC class I: a molecular basis for the presentation of transformed self. *Nat. Immunol.* 9, 1236–1243.

- Mohammed, F., Stones, D.H., Zarling, A.L., Willcox, C.R., Shabanowitz, J., Cummings, K.L., Hunt, D.F., Cobbold, M., Engelhard, V.H., Willcox, B.E., 2017. The antigenic identity of human class I MHC phosphopeptides is critically dependent upon phosphorylation status. *Oncotarget* 8, 54160–54172.
- Murshudov, G.N., Skubák, P., Lebedev, A.A., Pannu, N.S., Steiner, R.A., Nicholls, R.A., Winn, M.D., Long, F., Vagin, A.A., 2011. REFMAC5 for the refinement of macromolecular crystal structures. *Acta Crystallogr. D Biol. Crystallogr.* 67, 355–367.
- Ostrov, D.A., Grant, B.J., Pompeu, Y.A., Sidney, J., Harndahl, M., Southwood, S., Oseroff, C., Lu, S., Jakoncic, J., de Oliveira, C.A.F., Yang, L., Mei, H., Shi, L., Shabanowitz, J., English, A.M., Wriston, A., Lucas, A., Phillips, E., Mallal, S., Grey, H.M., Sette, A., Hunt, D.F., Buus, S., Peters, B., 2012. Drug hypersensitivity caused by alteration of the MHC-presented self-peptide repertoire. *Proc. Natl. Acad. Sci.* 109, 9959–9964.
- Petersen, J., Wurzbacher, S.J., Williamson, N.A., Ramarathinam, S.H., Reid, H.H., Nair, A.K.N., Zhao, A.Y., Nastovska, R., Rudge, G., Rossjohn, J., Purcell, A.W., 2009. Phosphorylated self-peptides alter human leukocyte antigen class I-restricted antigen presentation and generate tumor-specific epitopes. *Proc. Natl. Acad. Sci.* 106, 2776–2781.
- Schrodinger, L.L.C., 2015. The PyMOL Molecular Graphics System. (Version 1.8).
- Shiroishi, M., Kuroki, K., Rasubala, L., Tsumoto, K., Kumagai, I., Kurimoto, E., Kato, K., Kohda, D., Maenaka, K., 2006. Structural basis for recognition of the nonclassical MHC molecule HLA-G by the leukocyte Ig-like receptor B2 (LILRB2/LIR2/ILT4/CD85d). *Proc. Natl. Acad. Sci. U. S. A.* 103, 16412–16417.
- Vagin, A., Teplyakov, A., 2010. Molecular replacement with MOLREP. *Acta Crystallogr. Sect. D* 66, 22–25.
- Walter, T.S., Meier, C., Assenberg, R., Au, K.-F., Ren, J., Verma, A., Nettleship, Joanne E., Owens, R.J., Stuart, David I., Grimes, J.M., 2006. Lysine methylation as a routine rescue strategy for protein crystallization. *Structure* 14, 1617–1622.
- Warke, A., Momany, C., 2007. Addressing the protein crystallization bottleneck by cocrystallization. *Cryst. Growth Des.* 7, 2219–2225.
- Willcox, B.E., Thomas, L.M., Bjorkman, P.J., 2003. Crystal structure of HLA-A2 bound to LIR-1, a host and viral major histocompatibility complex receptor. *Nat. Immunol.* 4, 913–919.
- Winn, M.D., Ballard, C.C., Cowtan, K.D., Dodson, E.J., Emsley, P., Evans, P.R., Keegan, R.M., Krissinel, E.B., Leslie, A.G.W., McCoy, A., McNicholas, S.J., Murshudov, G.N., Pannu, N.S., Potterton, E.A., Powell, H.R., Read, R.J., Vagin, A., Wilson, K.S., 2011. Overview of the CCP4 suite and current developments. *Acta Crystallogr. D Biol. Crystallogr.* 67, 235–242.
- Zarling, A.L., Ficarro, S.B., White, F.M., Shabanowitz, J., Hunt, D.F., Engelhard, V.H., 2000. Phosphorylated peptides are naturally processed and presented by major histocompatibility complex class I molecules in vivo. *J. Exp. Med.* 192, 1755–1762.
- Zarling, A.L., Polefrone, J.M., Evans, A.M., Mikesch, L.M., Shabanowitz, J., Lewis, S.T., Engelhard, V.H., Hunt, D.F., 2006. Identification of class I MHC-associated phosphopeptides as targets for cancer immunotherapy. *Proc. Natl. Acad. Sci. U. S. A.* 103, 14889–14894.